Fast Surface Interpolation Using Multiresolution Wavelet Transform

Ming-Haw Yaou and Wen-Thong Chang

Abstract— **Discrete formulation of the surface interpolation problem usually leads to a large sparse linear equation system. Due to the poor convergence condition of the equation system, the convergence rate of solving this problem with iterative method is very slow. To improve this condition, a multiresolution basis transfer scheme based on the wavelet transform is proposed. By applying the wavelet transform, the original interpolation basis is transformed into two sets of bases with larger supports while the admissible solution space remains unchanged. With this basis transfer, a new set of nodal variables results and an equivalent equation system with better convergence condition can be solved. The basis transfer can be easily implemented by using an QMF matrix pair associated with the chosen interpolation basis. The consequence of the basis transfer scheme can be regarded as a preconditioner to the subsequent iterative computation method. The effect of the transfer is that the interpolated surface is decomposed into its low-frequency and high-frequency portions in the frequency domain. It has been indicated that the convergence rate of the interpolated surface is dominated by the low-frequency portion. With this frequency domain decomposition, the low-frequency portion of the interpolated surface can be emphasized. As compared with other acceleration methods, this basis transfer scheme provides a more systematical approach for fast surface interpolation. The easy implementation and high flexibility of the proposed algorithm also make it applicable to various regularization problems.**

Index Terms—**Surface interpolation, regularization, discretization, wavelet transform, basis transfer scheme, preconditioning.**

I. Introduction

SURFACE interpolation is to recover a full surface representation when only partial information of the surface is available. This problem plays an important role in many early vision processes such as surface from contours, shape from shading, structure from motion, stereopsis and so on [4], [9], [11], [16], [28], [37], [38]. This is an inverse and ill-posed problem. Regularization [12], [24], [36] is usually applied to make it well-posed. Then, various methods [10], [17], [35] can be used to discretize the problem into an objective function of discrete nodal variables such that an approximated solution which can be solved numerically is possible. It is known that the discrete formulation of the interpolation problem usually leads to a large sparse linear equation system. Hence, the iterative methods which require less storage in computation are usually adopted. However, due to the sparse system matrix of the resultant equation system, the convergence rate of the conventional iterative methods for solving this problem is very slow.

To speed up the convergence, acceleration methods such as multi-grid method [35], [37] and multilayer method [20] have been proposed. In those methods, the discretized problem is converted into a series of coarse subproblems with smaller grid sizes. With smaller size and denser structure system matrices, the convergence condition is improved. However, in these computation structures, the transfer between the adjoining subproblems is not straightforward and requires additional computational cost. In Szeliski [34], a preconditioning technique using hierarchical basis [39] was applied to improve the convergence rate. In his approach, the triangular nodal basis arising from the finite element method is partially replaced by a set of triangular functions with larger supports while the total number of interpolation nodes remains unchanged. The reorganization of nodal basis converts the interpolation problem into a new one with system matrix of lower condition number such that a better convergence condition can be obtained. Compared with those multi-grid like methods, the hierarchical basis method seems to be a easier algorithm for fast surface interpolation.

Basically, both the multigrid method and the hierarchical basis method utilize the multiresolution concept in improving the convergence rate. In the surface interpolation, the problem is to find a smooth surface which satisfies the constraints in the given nodes. In the equation system to be solved, the issues of constraint satisfaction and smoothness requirement are considered simultaneously during the iterative solving process. The global smoothness is established with a local relaxation manner. If the grid size is too fine and the support of basis is small, the convergence rate is usually very slow. Representation of the interpolation problem in different resolutions will increase the nodal connection such that the steady state can be reached faster. Since, in coarser resolution (with basis of larger support), larger connection between the nodal variables can be made in each iteration.

For a smooth surface, the global smoothness is largely dominated by the low-frequency portion. To indicate this, the difference between the temporary solution in each iteration and the true solution is analyzed. The difference is decomposed into its low-frequency and high-frequency portions. In our simulation, we have shown that the small attenuation speed of the low-frequency portion of the difference is the major reason of the slow convergence of the computation. Thus, a proper

Manuscript received March 15, 1993; revised December 6, 1993. This work was supported by the National Science Council, Republic of China, under Contract NSC83-0404-E-009-064. Recommended for acceptance by Associate Editor J. Daugman.

The authors are with the Institute of Communication Engineering and Center for Telecommunication Research, National Chiao Tung University, Hsinchu, Taiwan 30039, R.O.C.; e-mail: WTChang@TWNCTU01.

IEEE Log Number 9401648.

multiresolution scheme which can effectively manipulate the frequency domain property of the interpolation problem will be very helpful. Under this consideration, the multiresolution wavelet transform [5], [8], [26], [27], [33] becomes a better choice than those previously developed methods.

With the wavelet transform, the solution space of the interpolation problem can be decomposed into its low resolution subspace and the complementary detail subspaces. In the frequency domain, this vector space decomposition is equivalent to dividing the spectrum into low-frequency portion and high-frequency portion. Hence, the frequency domain property of the interpolation problem can be effectively manipulated. The vector space decomposition is performed by transferring the original interpolation basis into new sets of basis functions to define the low resolution subspace and the detail subspaces, respectively. These bases are generated by dilating and translating two prototype functions called the scaling function and wavelet. The basis transfer can be easily implemented with an QMF (quadrature mirror filter banks) matrix pair associated with the interpolation basis. Various interpolation bases have been investigated under this transform. Recently, the B-spline functions have been shown to be suitable for the surface interpolation [1], [6], [7].

In this paper, we utilize vector space decomposition/reconstruction theory of the wavelet transform to analyze the multiresolution representation of the surface interpolation problem. Through this analysis, an alternative multiresolution scheme to accelerate the convergence of iterative method is proposed. To describe the surface as a linear combination of the approximation basis, the Rayleigh–Ritz method [25], [32] is applied in our approach to discretize the variation functional associated with the regularized surface interpolation problem. Compared with other discretization methods, the advantage of such discretization is that the concept of signal approximation by weighted basis functions can be clearly stated. After the discretization, the basis transfer scheme based on the wavelet transform is used to transfer the chosen basis into two sets of bases with larger supports. The consequence of such basis transfer is a preconditioning of the associated equation system. To improve the convergence condition of a linear equation system by preconditioning has been an interesting issue. In this surface interpolation, we demonstrate how to construct the precondition matrix by the technique of basis transfer. With this, a fast interpolation can then be achieved by proper preconditioning of the equation system for any chosen iterative computation method.

To present our basis transfer scheme, the mathematical formulation of surface interpolation problem is briefly reviewed in Section II. Then, in Section III, the multiresolution wavelet transform is introduced. The basis transfer scheme based on the wavelet transform is described in detail. In Section IV, an asynchronous iterative computation method is derived. By applying the proposed basis transfer scheme as a preconditioner to the iterative computation method, the algorithm for fast surface interpolation is presented. In Section V, the results of experiments are shown and the performances of different acceleration methods are compared. Finally, a conclusion is given in Section 6.

II. The Surface Interpolation Problem

A. Regularization and Discretization

Surface interpolation is to recover a full surface representation when only partial information of the surface is available. Those available data are referred to as the constraints of the surface being interpolated. It is ill-posed since there are innumerable surfaces that can satisfy a given set of constraints. Hence, a regularization procedure considering the computation efficiency and visual relevance is usually applied. It has been a common approach to use variation functional [19], [36] to constrain the solution. The problem is usually formulated in the following form:

$$\mathcal{E}(f) = \mathcal{S}(f) + \beta \mathcal{C}(f). \tag{1}$$

The solution is the one that minimizes the objective functional $\mathcal{E}(f)$. The objective functional $\mathcal{E}(f)$ is the combination of a stabilizing functional $\mathcal{S}(f)$ and a cost functional $\mathcal{C}(f)$. The parameter β is non-negative and is used to adjust the weighting between the two considerations. The stabilizing functional $\mathcal{S}(f)$ is to set the smoothness constraint of the surface. It is usually defined in a quadratic form as

$$\mathcal{S}(f) \triangleq \int\int_{\Omega} (\mathcal{D}_x^2 f)^2 + 2(\mathcal{D}_x \mathcal{D}_y f)^2 + (\mathcal{D}_y^2 f)^2 d\Omega \tag{2}$$

where $\mathcal{D}_x$ and $\mathcal{D}_y$ are the differential operators with respect to x and y, respectively, and Ω is the domain of interest. The cost functional is to take into account the given constraints. For a surface denoted as $f(x, y)$ with constraints given in the form: $f(x_i, y_j) = q_{ij}$, for $(x_i, y_j) \in C_p$ and $q_{ij} \in C_d$, where $C_p \triangleq \{(x_i, y_j)\}|$ *at which point the constraints are given*$\}$ and $C_d \triangleq \{q_{ij}|$ *the known depth value at* $(x_i, y_j) \in C_p\}$, a commonly used cost functional is the following quadratic form,

$$\mathcal{C}(p) = \sum_{(x_i, y_j) \in C_p} [f(x_i, y_j) - q_{ij}]^2. \tag{3}$$

Through the above regularization, uniqueness of the solution of the problem can be guaranteed. The analytical solution of this optimization problem is difficult to obtain. Thus, an approximated solution which can be solved numerically is to be sought. In [10], Grimson used the finite difference to approximate the differential operators. In [35], Terzopoulos used finite element method to deduce a system of equations from which an alternative solution is solved. In this paper, the Rayleigh–Ritz [25], [32] method is used to define the admissible space from which the solution is derived. The advantage of such discretization is that the concept of signal approximation by weighted basis functions can be clearly stated. This can be useful in the latter discussion of multiresolution basis transfer scheme. We confine the admissible space to a N^2 dimensional function space spanned by a set of finitely supported bases. The surface in this space can be expressed by

$$f(x, y) = \sum_{i=0}^{N-1} \sum_{j=0}^{N-1} v_{ij} \Phi_{ij}(x, y), \tag{4}$$

where Φ_{ij}'s are the basis of the space $\mathbf{V} = \mathbf{span}\{\Phi_{0,0}, \Phi_{0,1}, \cdots, \Phi_{0,N-1}, \Phi_{1,0}, \cdots, \Phi_{N-1,N-1}\}$. The v_{ij}'s are the weighting coefficients. Substituting (4) into (2) and (3), the objective functional $\mathcal{E}(f)$ can be rewritten as

$$\mathcal{E} = \sum_{i=0}^{N-1}\sum_{j=0}^{N-1}\sum_{m=0}^{N-1}\sum_{n=0}^{N-1} v_{ij}t_{ijmn}v_{mn} + \beta \sum_{(x_i,y_j)\in C_p}\left[\sum_{m=0}^{N-1}\sum_{n=0}^{N-1} v_{mn}\Phi_{mn}(x_i,y_j) - q_{ij}\right]^2, \tag{5}$$

where quantity t_{ijmn} is defined as

$$t_{ijmn} \triangleq \int\int_{\Omega} (\mathcal{D}_x^2\Phi_{ij})(\mathcal{D}_x^2\Phi_{mn}) + 2(\mathcal{D}_x\mathcal{D}_y\Phi_{ij})(\mathcal{D}_x\mathcal{D}_y\Phi_{mn}) + (\mathcal{D}_y^2\Phi_{ij})(\mathcal{D}_y^2\Phi_{mn})d\Omega. \tag{6}$$

The quantity t_{ijmn} can be called relation coefficient because it describes the relation between variables v_{ij} and v_{mn}. As those basis functions spanning the admissible space are determined, all the relation coefficients can be determined via (6). Various types of the interpolation basis function can be used for this problem. In this paper, we select the tensor product of the tent functions (first-order B-spline basis) to span the solution space. B-spline basis [23] has been very popular for interpolation problem. In [18], B-spline basis of arbitrary order has been successfully applied for curve description. The 1-D tent function $\phi_i(x)$ located at $x = i$ with support 2 is defined by

$$\phi_i(x) \triangleq \begin{cases} x-1 & i-1 \le x < i \\ 1-x & i \le x < i+1 \\ 0 & \text{otherwise.} \end{cases}$$

In accordance with the tensor product method [23], [31], we set $\Phi_{ij}(x,y) = \phi_i(x)\phi_j(y)$. From the definition of tent function, it can be seen that

$$\Phi_{mn}(i,j) = \begin{cases} 1 & \text{for } i=m, j=n \\ 0 & \text{otherwise.} \end{cases}.$$

With this cardinal property of the tent function, Eq. (5) can be stated as

$$\mathcal{E} = \sum_{i=0}^{N-1}\sum_{j=0}^{N-1}\sum_{m=0}^{N-1}\sum_{n=0}^{N-1} v_{ij}t_{ijmn}v_{mn} + \beta \sum_{(i,j)\in C_i}[v_{ij} - q_{ij}]^2.$$

where $C_i = \{(i,j)|(i,j) = (x_i,y_j) \in C_p\}$. To unify the formula, we define

$$\beta_{ij} \triangleq \begin{cases} \beta & (i,j) \in C_i \\ 0 & \text{otherwise} \end{cases}$$

$$q_{ij} \triangleq \begin{cases} q_{ij} & (i,j) \in C_i \\ 0 & \text{otherwise.} \end{cases}$$

With these, we get

$$\mathcal{E} = \sum_{i=0}^{N-1}\sum_{j=0}^{N-1}\sum_{m=0}^{N-1}\sum_{n=0}^{N-1} v_{ij}t_{ijmn}v_{mn} + \sum_{i=0}^{N-1}\sum_{i=0}^{N-1}\beta_{ij}[v_{ij} - q_{ij}]^2, \tag{7}$$

Through this discretization, the interpolation problem can be expressed as the minimization of an objective function $\mathcal{E}$ of N^2 nodal variables v_{ij}'s.

B. Computational Considerations

The unknowns v_{ij}'s that minimize $\mathcal{E}$ can be solved from the Euler-Lagrange equation:

$$\frac{\partial \mathcal{E}}{\partial v_{ij}} = 0, \qquad \text{for all } v_{ij}. \tag{8}$$

Differentiation of (7) w.r.t. v_{ij}'s, the following set of equations result:

$$\sum_{m=0}^{N-1}\sum_{n=0}^{N-1} t_{ijmn}v_{mn} + \beta_{ij}[v_{ij} - q_{ij}] = 0. \quad 0 \sim i,j \sim N-1. \tag{9}$$

Thus, a system of N^2 simultaneous equations need to be solved for the surface interpolation. By concatenating all the nodal variables v_{ij}'s into one column vector $\mathbf{v}$, the above linear equation system can be expressed in its matrix form as

$$\mathbf{Av} - \mathbf{b} = 0. \tag{10}$$

where the system matrix $\mathbf{A}$ is a $N^2 \times N^2$ matrix defined as the matrix found at the bottom of the page. The vector $\mathbf{b}$ is defined as

$$\mathbf{b} \triangleq [\beta_{0,0}q_{0,0}\beta_{0,1}q_{0,1}\cdots\beta_{0,N-1}q_{0,N-1}\beta_{1,N-1}q_{1,N-1}\cdots\cdots \beta_{N-1,N-1}q_{N-1,N-1}]^T.$$

Hence, through the regularization and discretization, the surface interpolation can be formalized as a linear equation system. The problem is to solve those variables $\mathbf{v}$ such that the equation system can be satisfied. It is easy to see, even for a surface of median size, the size of the system matrix

$$\mathbf{A} \triangleq \begin{bmatrix} t_{0,0,0,0}+\beta_{0,0} & t_{0,0,0,1} & t_{0,0,0,2} & \cdots & \cdots & \cdots & t_{0,0,N-1,N-1} \\ t_{0,1,0,0} & t_{0,1,0,1}+\beta_{0,1} & t_{0,1,0,2} & \cdots & \cdots & \cdots & t_{0,1,N-1,N-1} \\ t_{0,2,0,0} & t_{0,2,0,1} & t_{0,2,0,2}+\beta_{0,2} & \cdots & \cdots & \cdots & t_{0,2,N-1,N-1} \\ \vdots & \vdots & \vdots & \ddots & & \cdots & \vdots \\ \vdots & \vdots & \vdots & & \ddots & & \vdots \\ t_{N-1,N-2,0,0} & t_{N-1,N-2,0,1} & t_{N-1,N-2,0,2} & \cdots & & \ddots & t_{N-1,N-2,N-1,N-1} \\ t_{N-1,N-1,0,0} & t_{N-1,N-1,0,1} & t_{N-1,N-1,0,2} & \cdots & \cdots & \cdots & t_{N-1,N-1,N-1,N-1}+\beta_{N-1,N-1} \end{bmatrix}$$

A will be very large. Hence, in solving this problem, the iterative methods are usually adopted instead of the direct solving method.

It can be found that the equation system is characterized by the system matrix **A**. The computation speed of the equation system with iterative methods will be directly affected by the structure of matrix **A**. In the surface interpolation problem, the given constraints are usually sparse. Most of the parameters β_{ij} are zero except those associated to the nodes with given constraints. Hence, the variance of the diagonal elements in matrix **A** is often large. Also, due to the finite support of the interpolation basis, most of the off-diagonal elements in matrix **A** (i.e., $t_{ijmn,(i\neq m,j\neq n)}$) are zero. This causes a very sparse structure of matrix **A**. These characteristics of the system matrix make the equation system nearly singular and result in a poor convergence condition when solving the equation system with iterative methods. The sparse structure of matrix **A** indicates that the connection among the variables v_{ij}'s is very low. Since, for a variable v_{ij}, most of the relation coefficients t_{ijmn}'s which relate v_{ij} to other nodal variables v_{mn}'s are zero. In the iterative solving methods, this local connection will slow down the progress of the solution in iteration and result in a low convergence rate.

To obtain a fast surface interpolation, a proper scheme which can transfer the equation system to a better condition is necessary. In the past, the multi-grid method [35], [37] and the multi-layer method [20] have been successfully applied to speed up the convergence. In those approaches, the coarse versions of the original interpolated surface are extracted. The steady state solutions of the coarse versions are then used as the initial condition for the original domain to expedite the computation. However, the complicated computation structure of those methods makes them inefficient to be implemented. An alternative approach which is easier to implement has been proposed by Szeliski [34]. In Szeliski's approach, the preconditioning scheme proposed by Yserntant [39] was applied. The linear equation system associated with the surface interpolation problem is preconditioned by replacing the nodal basis with a hierarchy of basis functions with larger supports. The replacement of nodal basis can reduce the condition number of the system matrix such that a better convergence condition can be obtained.

The basic concept of those previously developed methods is to solve the interpolation problem in different resolutions. For example, the basis replacement scheme used in Szeliski's approach can be interpreted as a signal representation in different resolution levels. Since, the expansion of signal with dilated basis functions is equivalent to the representation of signal in coarser resolution space. This observation indicates that the acceleration of interpolation can be analyzed from the multiresolution point of view. In the frequency domain, the coarse resolution version of a signal can be interpreted as the low-frequency component in spectrum. As the low resolution version can be obtained by approximating a signal with the dilated version of the original basis functions, it should be possible to obtain the complementary high-frequency portions from the complementary subspace of the coarse resolution subspace. The complete information of the low-frequency and high-frequency components can be quite useful in designing an effective multiresolution scheme for fast computation. Since, from the local Fourier analysis [3], [14], [13], it is found that the computation speed of surface interpolation is dominated by the low-frequency portion of the interpolation problem. Hence, a proper multiresolution scheme which can effectively manipulate the frequency domain property to emphasize the attenuation of the low-frequency will expedite the interpolation speed.

In the past, acceleration schemes based on the multiresolution concept have been utilized. However, the frequency domain property of the interpolation problem was not effectively utilized in those methods. For effectively utilizing the multiresolution concept, a multiresolution scheme which can effectively manipulate the frequency domain property is proposed. In the following sections, an alternative acceleration method based on the basis transfer scheme by wavelet transform [8], [5], [7], [26], [33] is introduced.

III. Basis Transfer Scheme Using Wavelet Transform

A. Multiresolution Wavelet Transform

The basic idea of wavelet transform is to represent a continuous function $F(x)$ as the limit of successive approximations, each of which is a smoothed version of $F(x)$. The transform is performed by using a set of bases $\phi_{mn}(x)$ to expand the continuous function $F(x)$. These bases are generated by dilating and translating a prototype function $\phi(x)$ called the scaling function. Also, the difference between two approximations can be obtained by expanding the signal with another set of bases $\psi_{mn}(x)$ which is generated by another prototype function $\psi(x)$ called the wavelet. The wavelet transform can be expressed as

$$P_m F = \sum_n f_m[n]\phi_{mn}(x)_{\cdot(m,n\in\mathcal{Z})}$$

$$\phi_{mn}(x) \triangleq 2^{\frac{-m}{2}}\phi(2^{-m}x - n). \tag{11}$$

$$Q_m F = \sum_n d_m[n]\psi_{mn}(x)_{\cdot(m,n\in\mathcal{Z})}$$

$$\psi_{mn}(x) \triangleq 2^{\frac{-m}{2}}\psi(2^{-m}x - n). \tag{12}$$

The signal $P_m F$ is the approximation of $F(x)$ at resolution m (smaller m corresponds to higher resolution). The signal $Q_m F$ is the differences between approximations $P_{m-1}F$ and $P_m F$. Note that the approximation bases $\phi_{mn}(x)$ and $\psi_{mn}(x)$ at different resolutions are of the same shape but in different scales. Hence, a signal can be approximated in different resolution levels by using the different scaled versions of an identical basis function.

Assume that the original signal is defined at the resolution level 0, i.e., $F(x) = P_0 F$, then a multiresolution representation of the signal $F(x)$ can be established by applying the wavelet transform in different resolution levels. As described in Fig. 1, a signal $F(x)$ can be represented as a pyramidal structure consisting of its lower resolution versions $P_i F$ and details $Q_i F_{,(i=1,2,\cdots)}$. According to the vector projection theory, this multiresolution signal representation is based on

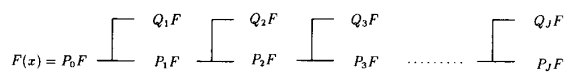

Fig. 1. The multiresolution representation of the continuous signal $F(x)$.

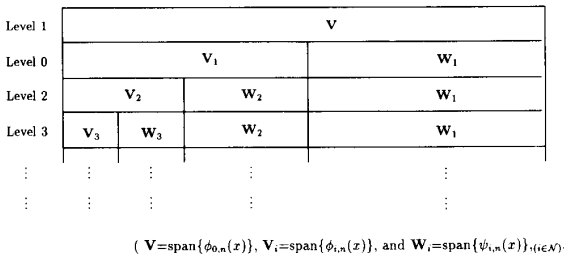

Fig. 2. The vector space decomposition in wavelet transform.

the recursive subdivision of the signal vector space. Define the vector space spanned by the basis $\phi_{0n}(x)$ as $\mathbf{V}$, then the approximation P_iF is equivalent to projecting the signal $F(x)$ onto the subspace $\mathbf{V}_i$ of space $\mathbf{V}$, and the detail Q_iF is the projection of $F(x)$ onto the complementary subspace $\mathbf{W}_i$ of subspace $\mathbf{V}_i$. This vector space decomposition is described in Fig. 2. As long as the bases $\phi_{mn}(x)$ and $\psi_{mn}(x)$ are designed according to this complementary vector space property, a signal can be represented in any desired levels of approximations.

In wavelet transform, the weighting sequences $f_m[n]$ and $d_m[n]$ in (11) and (12) play an important role in multiresolution analysis. The wavelet transform can be exactly characterized by these discrete signals. This discrete property maps the analysis from the continuous signal space onto the discrete signal space and provides a powerful tool to deal with sampled signals. The transformation between a discrete sequence $f_m[n]$ and its lower resolution sequences $f_{m+1}[n]$ and $d_{m+1}[n]$ can be expressed as, for $m = 0, 1, 2, \cdots$,

$$f_{m+1}[n] = \sum_k h_0[k-2n] f_m[k],$$
$$d_{m+1}[n] = \sum_k h_1[k-2n] f_m[k]. \tag{13}$$

$$f_m[n] = \sum_k f_{m+1}[k] g_0[n-2k] + \sum_k d_{m+1}[k] g_1[n-2k], \tag{14}$$

where the sequences $h_i[n]$ and $g_i[n]_{,(i=0,1)}$ can be derived from the functions $\phi(x)$ and $\psi(x)$. It has been indicated [8], [7], [26] that this discrete wavelet transform can be implemented in an QMF structure as described in Fig. 3. The sequences $h_i[n]$ and $g_i[n]$ can be interpreted as the analysis and the synthesis filters of a filter banks. Denoting the discrete sequences $f_m[n]$, $f_{m+1}[n]$, and $d_{m+1}[n]$ as vectors $\mathbf{f}_m$, $\mathbf{f}_{m+1}$, and $\mathbf{d}_{m+1}$, the filter banks structure of the discrete wavelet transform can be formulated in its matrix form as, for $m = 0, 1, 2, \cdots$,

$$\mathbf{f}_{m+1} = \mathbf{H}_0^{\frac{N}{2^m}} \mathbf{f}_m, \qquad \mathbf{d}_{m+1} = \mathbf{H}_1^{\frac{N}{2^m}} \mathbf{f}_m. \tag{15}$$
$$\mathbf{f}_m = \mathbf{G}_0^{\frac{N}{2^m}} \mathbf{f}_{m+1} + \mathbf{G}_1^{\frac{N}{2^m}} \mathbf{d}_{m+1}, \tag{16}$$

where the matrices $\mathbf{H}_i^{\frac{N}{2^m}}$ and $\mathbf{G}_i^{\frac{N}{2^m}}{}_{,(i=0,1)}$ are defined as (17) and (18) found at the bottom of the page where the superscript $\frac{N}{2^m}$ is used to describe the size of the matrix. If the length of vector $\mathbf{f}_0$ is N, then $\mathbf{H}_i^{\frac{N}{2^m}}$ and $\mathbf{G}_i^{\frac{N}{2^m}}$ will be circulant matrices[1] of size $\frac{N}{2^{m+1}} \times \frac{N}{2^m}$ and $\frac{N}{2^m} \times \frac{N}{2^{m+1}}$, respectively. The length of vectors $\mathbf{f}_{m+1}$ and $\mathbf{d}_{m+1}$ will be half of the length of vector $\mathbf{f}_m$. Applying this decomposition repeatedly, a discrete multiresolution signal representation corresponding to the discrete wavelet transform can be obtained as described in Fig. 4. This decomposition which represents a signal $\mathbf{f}_0$ in its J levels lower resolution versions $\{\mathbf{f}_J, \mathbf{d}_{j,(j=1\sim J)}\}$ is called the multiresolution wavelet representation [26]

B. Basis Transfer Scheme

It can be found that the signal approximation by basis expansion in the wavelet transform has the same form as the Rayleigh-Ritz method used in the discretization of the interpolation problem. If we treat the Rayleigh–Ritz method described

[1] This circulant matrix representation is obtained by using circular convolution in the filtering process. The filters $h_i[n]$ and $g_i[n]$ are usually FIR filters and have filter length less than $\frac{N}{2^m}$. The sequences $h_i[n]$ and $g_i[n]$ inside the matrices $\mathbf{H}_i^{\frac{N}{2^m}}$ and $\mathbf{G}_i^{\frac{N}{2^m}}$ are expressed in their zero-padding forms.

$$\mathbf{H}_i^{\frac{N}{2^m}} \triangleq \begin{bmatrix} h_i[0] & h_i[\frac{N}{2^m}-1] & h_i[\frac{N}{2^m}-2] & h_i[\frac{N}{2^m}-3] & \cdots & \cdots & h_i[2] & h_i[1] \\ h_i[2] & h_i[1] & h_i[0] & h_i[\frac{N}{2^m}-1] & \cdots & \cdots & h_i[4] & h_i[3] \\ h_i[4] & h_i[3] & h_i[2] & h_i[1] & \cdots & \cdots & h_i[6] & h_i[5] \\ \vdots & \vdots & \vdots & \vdots & \vdots & \vdots & \vdots & \vdots \\ \vdots & \vdots & \vdots & \vdots & \vdots & \vdots & \vdots & \vdots \\ h_i[\frac{N}{2^m}-2] & h_i[\frac{N}{2^m}-3] & h_i[\frac{N}{2^m}-4] & h_i[\frac{N}{2^m}-5] & \cdots & \cdots & h_i[0] & h_i[\frac{N}{2^m}-1] \end{bmatrix} \tag{17}$$

$$\mathbf{G}_i^{\frac{N}{2^m}} \triangleq \begin{bmatrix} g_i[0] & g_i[1] & g_i[2] & g_i[3] & \cdots & \cdots & g_i[\frac{N}{2^m}-2] & g_i[\frac{N}{2^m}-1] \\ g_i[\frac{N}{2^m}-2] & g_i[\frac{N}{2^m}-1] & g_i[0] & g_i[1] & \cdots & \cdots & g_i[\frac{N}{2^m}-4] & g_i[\frac{N}{2^m}-3] \\ g_i[\frac{N}{2^m}-4] & g_i[\frac{N}{2^m}-3] & g_i[\frac{N}{2^m}-2] & g_i[\frac{N}{2^m}-1] & \cdots & \cdots & g_i[\frac{N}{2^m}-6] & g_i[\frac{N}{2^m}-5] \\ \vdots & \vdots & \vdots & \vdots & \vdots & \vdots & \vdots & \vdots \\ \vdots & \vdots & \vdots & \vdots & \vdots & \vdots & \vdots & \vdots \\ g_i[2] & g_i[3] & g_i[4] & g_i[5] & \cdots & \cdots & g_i[0] & g_i[1] \end{bmatrix}^T \tag{18}$$

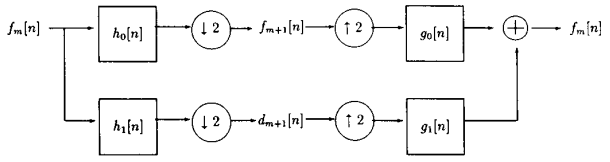

Fig. 3. The QMF structure of discrete wavelet transform.

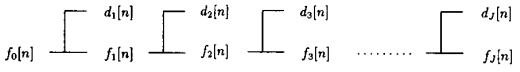

Fig. 4. The multiresolution representation of the discrete signal $f_0[n]$.

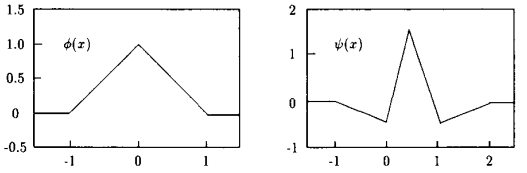

Fig. 5. The wavelet $\psi(x)$, scaling function $\phi(x)$, and the impluse responses of the associated QMF filters.

in (4) as a wavelet transform at resolution level 0, the B-spline function can then be interpreted as the scaling function $\phi(x)$. The nodal variables v_{ij}'s are equivalent to the discrete sequence $f_0[n]$. Wavelet transform using B-spline polynomial as scaling function has been studied in [7], [1], [6]. In [7], some examples of B-spline wavelet transform have been shown. Fig. 5 shows one set of the designed prototype functions and the associated QMF filters.[2] With these prototype functions and filters, a multiresolution representation of the interpolation problem can then be established by approximating the surface with the corresponding bases $\phi_{mn}(x)$ and $\psi_{mn}(x)$. The nodal variables can thus be represented in a pyramidal structure as shown in Fig. 4 by applying the discrete wavelet transform. Since the surface interpolation is a 2-D problem, a 2-D wavelet transform is necessary. This can be done by extending the 1-D wavelet transform by tensor product operation. If we define the nodal variables v_{ij}'s of a $N \times N$ surface interpolation problem as the highest resolution signal $\mathbf{v}$, then the multiresolution representation of it can be generated by recursively applying the 2-D discrete wavelet transform as

$$\mathbf{v}_{m+1} = \left(\mathbf{H}_0^{\frac{N}{2^m}} \otimes \mathbf{H}_0^{\frac{N}{2^m}}\right)\mathbf{v}_m, \mathbf{w}_{m+1}^1 = \left(\mathbf{H}_0^{\frac{N}{2^m}} \otimes \mathbf{H}_1^{\frac{N}{2^m}}\right)\mathbf{v}_m,$$
$$\mathbf{w}_{m+1}^2 = \left(\mathbf{H}_1^{\frac{N}{2^m}} \otimes \mathbf{H}_0^{\frac{N}{2^m}}\right)\mathbf{v}_m, \mathbf{w}_{m+1}^3 = \left(\mathbf{H}_1^{\frac{N}{2^m}} \otimes \mathbf{H}_1^{\frac{N}{2^m}}\right)\mathbf{v}_m.$$
$$m = 0, 1, 2, \cdots \quad (19)$$

$$\mathbf{v}_m = \left(\mathbf{G}_0^{\frac{N}{2^m}} \otimes \mathbf{G}_0^{\frac{N}{2^m}}\right)\mathbf{v}_{m+1} + \left(\mathbf{G}_0^{\frac{N}{2^m}} \otimes \mathbf{G}_1^{\frac{N}{2^m}}\right)\mathbf{w}_{m+1}^1$$
$$+ \left(\mathbf{G}_1^{\frac{N}{2^m}} \otimes \mathbf{G}_0^{\frac{N}{2^m}}\right)\mathbf{w}_{m+1}^2 + \left(\mathbf{G}_1^{\frac{N}{2^m}} \otimes \mathbf{G}_1^{\frac{N}{2^m}}\right)\mathbf{w}_{m+1}^3.$$
$$m = 0, 1, 2, \cdots \quad (20)$$

where the operator $\otimes$ stands for the matrix tensor product. In this 2-D case, a quartered multiresolution representation of the nodal variables v_{ij}'s is generated. As described in Fig. 6, each signal $\mathbf{v}_m$ is decomposed into its lower resolution version $\mathbf{v}_{m+1}$ and three detail components $\mathbf{w}_{m+1,(i=1,2,3)}^i$. The signal length of each decomposed signal is a quarter of that in the upper resolution level. Hence, the total signal length remains the same in each resolution levels. In this representation, the nodal variables in vector $\mathbf{v}$ are represented as $\{\mathbf{v}_J, \mathbf{w}_{j,(j=1\sim J,i=1,2,3)}^i\}$, where J is the level of resolution. From the vector space point of view, this multiresolution transform is equivalent to transferring the approximation basis from $\phi_{0n}(x)$ to $\{\phi_{Jn}, \psi_{jn,(j=1\sim J)}\}$, while the admissible signal space remains unchanged. The signals $\mathbf{v}_J$ and $\mathbf{w}_{j,(j=1\sim J,i=1,2,3)}^i$ are the weighting coefficients of the two sets of bases $\{\phi_{Jn}\}$ and $\{\psi_{jn,(j=1\sim J)}\}$, respectively. In the frequency domain, the low resolution signal $\mathbf{v}_J$ can be interpreted as the low-frequency version of the original nodal variables $\mathbf{v}$. And the details $\mathbf{w}_{j,(j=1\sim J,i=1,2,3)}^i$ can be interpreted as the high-frequency components.

If the signals $\{\mathbf{v}_J, \mathbf{w}_j^i\}$ are represented as a vector $\tilde{v}$, the conversion of $\mathbf{v}$ into $\tilde{\mathbf{v}}$ can be done by using an QMF matrix pair $\mathbf{D}$ and $\mathbf{R}$ as

$$\tilde{\mathbf{v}} = \mathbf{D}\mathbf{v}, \quad \mathbf{v} = \mathbf{R}\tilde{\mathbf{v}}, \quad \tilde{\mathbf{v}} \triangleq \begin{bmatrix} \mathbf{v}_J \\ \mathbf{w}_J^1 \\ \mathbf{w}_J^2 \\ \mathbf{w}_J^3 \\ \vdots \\ \mathbf{w}_1^1 \\ \mathbf{w}_1^2 \\ \mathbf{w}_1^3 \end{bmatrix} \quad (21)$$

where the matrices $\mathbf{D}$ and $\mathbf{R}$ can be derived as when $J = 1$:

$$\mathbf{D} = \begin{bmatrix} \mathbf{H}_0^N \\ \mathbf{H}_1^N \end{bmatrix} \otimes \begin{bmatrix} \mathbf{H}_0^N \\ \mathbf{H}_1^N \end{bmatrix}$$
$$\mathbf{R} = \begin{bmatrix} (\mathbf{G}_0^N)^T \\ (\mathbf{G}_1^N)^T \end{bmatrix}^T \otimes \begin{bmatrix} (\mathbf{G}_0^N)^T \\ (\mathbf{G}_1^N)^T \end{bmatrix}^T \quad (22)$$

when $J = 2$:

$$\mathbf{D} = \begin{bmatrix} \mathbf{H}_0^{\frac{N}{2}}\mathbf{H}_0^N \\ \mathbf{H}_1^{\frac{N}{2}}\mathbf{H}_0^N \\ \mathbf{H}_1^N \end{bmatrix} \otimes \begin{bmatrix} \mathbf{H}_0^{\frac{N}{2}}\mathbf{H}_0^N \\ \mathbf{H}_1^{\frac{N}{2}}\mathbf{H}_0^N \\ \mathbf{H}_1^N \end{bmatrix}$$
$$\mathbf{R} = \begin{bmatrix} (\mathbf{G}_0^N\mathbf{G}_0^{\frac{N}{2}})^T \\ (\mathbf{G}_0^N\mathbf{G}_1^{\frac{N}{2}})^T \\ (\mathbf{G}_1^N)^T \end{bmatrix}^T \otimes \begin{bmatrix} (\mathbf{G}_0^N\mathbf{G}_0^{\frac{N}{2}})^T \\ (\mathbf{G}_0^N\mathbf{G}_1^{\frac{N}{2}})^T \\ (\mathbf{G}_1^N)^T \end{bmatrix}^T \quad (23)$$

[2]Here, QMF is used in a general sense to denote filter banks designed by both orthogonal and biorthogonal bases. Since, there is still no suitable terminology to distinguish these two cases.

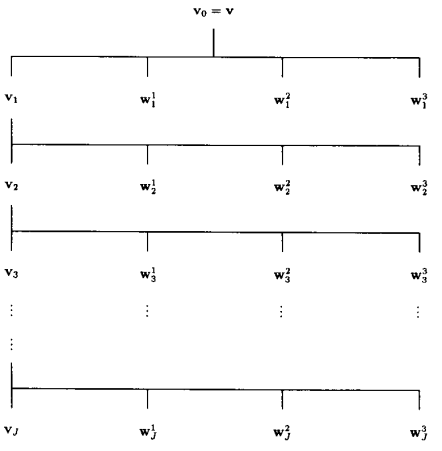

Fig. 6. The multiresolution representation of the nodal variables $\mathbf{v}$.

when $J \geq 3$:

$$\mathbf{D} \triangleq \begin{bmatrix} \mathbf{H}_0^{\frac{N}{2^{J-1}}} & \mathbf{H}_0^{\frac{N}{2^{J-2}}} & \cdots & \mathbf{H}_0^N \\ \mathbf{H}_1^{\frac{N}{2^{J-1}}} & \mathbf{H}_0^{\frac{N}{2^{J-2}}} & \cdots & \mathbf{H}_0^N \\ & \mathbf{H}_1^{\frac{N}{2^{J-2}}} & \cdots & \mathbf{H}_0^N \\ & & & \vdots \\ & & & \mathbf{H}_1^N \end{bmatrix} \otimes \begin{bmatrix} \mathbf{H}_0^{\frac{N}{2^{J-1}}} & \mathbf{H}_0^{\frac{N}{2^{J-2}}} & \cdots & \mathbf{H}_0^N \\ \mathbf{H}_1^{\frac{N}{2^{J-1}}} & \mathbf{H}_0^{\frac{N}{2^{J-2}}} & \cdots & \mathbf{H}_0^N \\ & \mathbf{H}_1^{\frac{N}{2^{J-2}}} & \cdots & \mathbf{H}_0^N \\ & & & \vdots \\ & & & \mathbf{H}_1^N \end{bmatrix} \tag{24}$$

$$R \triangleq \begin{bmatrix} (\mathbf{G}_0^N & \cdots & \mathbf{G}_0^{\frac{N}{2^{J-2}}} & \mathbf{G}_0^{\frac{N}{2^{J-1}}})^T \\ (\mathbf{G}_0^N & \cdots & \mathbf{G}_0^{\frac{N}{2^{J-2}}} & \mathbf{G}_1^{\frac{N}{2^{J-1}}})^T \\ (\mathbf{G}_0^N & \cdots & \mathbf{G}_1^{\frac{N}{2^{J-2}}})^T & \\ \vdots & & & \\ (\mathbf{G}_1^N)^T & & & \end{bmatrix}^T \otimes \begin{bmatrix} (\mathbf{G}_0^N & \cdots & \mathbf{G}_0^{\frac{N}{2^{J-2}}} & \mathbf{G}_0^{\frac{N}{2^{J-1}}})^T \\ (\mathbf{G}_0^N & \cdots & \mathbf{G}_0^{\frac{N}{2^{J-2}}} & \mathbf{G}_1^{\frac{N}{2^{J-1}}})^T \\ (\mathbf{G}_0^N & \cdots & \mathbf{G}_1^{\frac{N}{2^{J-2}}})^T & \\ \vdots & & & \\ (\mathbf{G}_1^N)^T & & & \end{bmatrix}^T \tag{25}$$

where the matrices $\mathbf{H}_i^{\frac{N}{2^j}}$ and $\mathbf{G}_i^{\frac{N}{2^j}}$ are those described in (17) and (18). As long as the interpolation basis is chosen, the matrices $\mathbf{D}$ and $\mathbf{R}$ can be easily derived according to the above formulations. For the equation system $\mathbf{A}\mathbf{v} - \mathbf{b} = 0$ derived in the discretization procedure in the previous section, it is easy to show that the solution to be sought is to minimize the energy function

$$\frac{1}{2}\mathbf{v}^T\mathbf{A}\mathbf{v} - \mathbf{v}^T\mathbf{b}. \tag{26}$$

By converting the nodal variables $\mathbf{v}$ into $\tilde{\mathbf{v}}$, we can rewrite the energy function as

$$\frac{1}{2}(\mathbf{R}\tilde{\mathbf{v}})^T\mathbf{A}(\mathbf{R}\tilde{\mathbf{v}}) - (\mathbf{R}\tilde{\mathbf{v}})^T\mathbf{b}. \tag{27}$$

The minimization of this transferred energy function is equivalent to the solving of the following equation system

$$\tilde{\mathbf{A}}\tilde{\mathbf{v}} = \tilde{\mathbf{b}}, \qquad \text{where } \tilde{\mathbf{A}} \triangleq \mathbf{R}^T\mathbf{A}\mathbf{R}, \qquad \tilde{\mathbf{b}} \triangleq \mathbf{R}^T\mathbf{b}. \tag{28}$$

Hence, with this basis transfer scheme, the original equation system is transferred to an equivalent equation system with new nodal variables $\tilde{\mathbf{v}}$.

According to the time-scale property of the bases $\phi_{mn}(x)$ and $\psi_{mn}(x)$, the transferred bases will have larger supports. Since interpolation basis with larger region of support will reduce the zero elements in the relation coefficients t_{ijmn}'s, it can be verified that the new system matrix $\tilde{\mathbf{A}}$ will be denser than the original matrix $\mathbf{A}$. This implies that more global connection between the interpolation nodes can be made. Hence, a faster convergence can be obtained in the iterative solving method.

In the conversion of $\mathbf{v}$ into $\tilde{\mathbf{v}}$, the low-frequency component $\mathbf{v}_J$ and the high-frequency components $\mathbf{w}_j^i$,$(j=1\sim J, i=1,2,3)$ are extracted. This conversion allows the low-frequency portion and the high-frequency portion of the interpolation problem to be solved separately. In the iterative solving method, the solution is obtained by updating the nodal variables sequentially through a local relaxation process. The high-frequency portion which contains mainly local information usually converges fast. However, the low-frequency portion which contains the global structure of the surface will take much more computations to reach the steady state. Since the low-frequency portion is related to the global characteristics of the interpolated surface, a complete refinement of this portion can be achieved only after every nodal variable is updated. Thus, the low convergence rate is usually due to the slow refinement of the low-frequency portion. By applying the basis transfer scheme, the original nodal variables in vector $\mathbf{v}$ are converted to new variables $\{\mathbf{v}_J, \mathbf{w}_j^i\}$. The low-frequency portion of the interpolated surface is characterized by these variables in vector $\mathbf{v}_J$. These fewer variables are connected with bases of larger support, thus the refinement can be made very fast and the convergence rate can be improved.

With the above analysis, a fast surface interpolation can be achieved by simply applying the above basis transfer scheme as a preconditioner to the original equation system. This preconditioning scheme is similar to the hierarchical basis preconditioning method developed by Yeserentant [39]. Based on the multi-level splitting of finite element spaces, Yeserentant reorganized the original triangular basis functions into a hierarchy of triangular functions with larger supports. This hierarchical basis method has been successfully applied in

the surface interpolation problem [34]. The difference between the proposed basis transfer scheme and the hierarchical basis method is in their manipulation of the nodal basis. In the hierarchical basis method, the low resolution version and the details of the interpolated surface are not explicitly separated. The set of hierarchical bases used to replace the original nodal basis consists of a mixture of the bases with different regions of support. However, in the proposed basis transfer method, the original node basis is transferred into two sets of bases $\{\phi_{Jn}(x)\}$ and $\{\psi_{jn}(x)_{,(j=1\sim J)}\}$ which are generated from the scaling function $\phi(x)$ and the wavelet $\psi(x)$. These two sets of bases define the low resolution version and the details of the approximated signal.

As discussed previously, the low resolution version and details can be interpreted as the low-frequency component and the high-frequency components of the approximated signal. Hence, the basis transfer method can completely describe the frequency domain characteristics of the approximated signal. Also, different scaling functions and wavelets can provide different interpolation basis for surface interpolation beside the triangular function. This makes the proposed basis transfer method more flexible than the hierarchical basis method.

IV. Fast Surface Interpolation Algorithm

In the previous section, we have shown that the consequence of the basis transfer is the transform of the system matrix of the surface interpolation problem as described in (28). The purpose of this transformation is to change the structure of the system matrix in order to speed up the convergence rate in the iterative solving process. In this section, we will investigate the effect of this system transformation on the computation speed of an asynchronous iterative method which is used to derived the solution.

A. The Asynchronous Iterative Computation Method

In Section II, we have shown that the interpolation problem is to minimize the energy function $\mathcal{E}$. The asynchronous computation structure is derived based on the process to minimize this energy function. From (7) in Section II, if one of the variables, say $v_{i_0j_0}$, is assumed to vary by an amount $\Delta v_{i_0j_0}$, the value of the function $\mathcal{E}$ will vary by an amount $\Delta\mathcal{E}$, that is

$$\begin{aligned}\mathcal{E}+\Delta\mathcal{E} = &\sum_{\substack{i\\ ij\neq i_0j_0}}\sum_{j}\sum_{\substack{m\\ mn\neq i_0j_0}}\sum_{n} v_{ij}t_{ijmn}v_{mn}\\ &+2(v_{i_0j_0}+\Delta v_{i_0j_0})\sum_{\substack{m\\ mn\neq i_0j_0}}\sum_{n} t_{i_0j_0mn}v_{mn}\\ &+t_{i_0j_0i_0j_0}(v_{i_0j_0}+\Delta v_{i_0j_0})^2\\ &+\sum_{\substack{i\\ ij\neq i_0j_0}}\sum_{j}\beta_{ij}[v_{ij}-q_{ij}]^2\\ &+\beta_{i_0j_0}[v_{i_0j_0}+\Delta v_{i_0j_0}-q_{i_0j_0}]^2.\end{aligned}$$

The variation $\Delta\mathcal{E}$ is given by

$$\begin{aligned}\Delta\mathcal{E} = &(t_{i_0j_0i_0j_0}+\beta_{i_0j_0})\Delta v_{i_0j_0}^2\\ &+2\Delta v_{i_0j_0}\left[\sum_{m=0}^{N-1}\sum_{n=0}^{N-1} t_{i_0j_0mn}v_{mn}+\beta_{i_0j_0}(v_{i_0j_0}-q_{i_0j_0})\right].\end{aligned}$$

It can be found that $\Delta\mathcal{E}$ is a parabolic function of $\Delta v_{i_0j_0}$. Thus, with respect to $\Delta v_{i_0j_0}$, $\Delta\mathcal{E}$ can be made maximum when

$$\begin{aligned}\Delta v_{i_0j_0} = &\frac{-1}{t_{i_0j_0i_0j_0}+\beta_{i_0j_0}}\\ &\times\left[\sum_{m=0}^{N-1}\sum_{n=0}^{N-1} t_{i_0j_0mn}v_{mn}+\beta_{i_0j_0}(v_{i_0j_0}-q_{i_0j_0})\right]\end{aligned} \tag{29}$$

and the corresponding $\Delta\mathcal{E}$ is given by

$$\Delta\mathcal{E} = -(t_{i_0j_0i_0j_0}+\beta_{i_0j_0})\Delta v_{i_0j_0}^2. \tag{30}$$

From the definitions of t_{ijij} and β_{ij}, it is easy to see that $t_{ijij}+\beta_{ij}>0$ for all i,j. Hence, the value of $\mathcal{E}$ will decrease monotonously as each v_{ij} is updated according to (29). Also, the decrement of $\mathcal{E}$ is maximized with respect to the change of each variable. The computation continues until all $\Delta v_{i_0j_0}$'s reach zero such that the minimum of $\mathcal{E}$ is obtained. From Eq. (29), we can write the update formula as

$$v_{ij}^{(\text{new})} = \frac{-1}{t_{ijij}+\beta_{ij}}\left[\sum_{\substack{m\\ m,n\neq i,j}}\sum_{n} v_{mn}^{(\text{old})}t_{ijmn}-\beta_{ij}q_{ij}\right]. \tag{31}$$

where $v_{ij}^{(\text{new})}$ is the new value of v_{ij} and $v_{mn}^{(\text{old})}$'s are the values of the variables at the time when v_{ij} is updated. Recall the matrix representation used in Section II, the update formula can be expressed in the form as

$$\mathbf{v}_{(k)}^{\text{new}} = \frac{-1}{\mathbf{A}_{(k,k)}}\left[\sum_{l=0,l\neq k}^{N^2-1}\mathbf{A}_{(k,l)}\mathbf{v}_{(l)}^{\text{old}}-\mathbf{b}_{(k)}\right], \tag{32}$$

where $\mathbf{v}_{(k)}$ and $\mathbf{b}_{(k)}$ denote the k-th element in vector $\mathbf{v}$ and $\mathbf{b}$, respectively, and $\mathbf{A}_{(k,l)}$ denote the element of matrix $\mathbf{A}$ in position (k,l). Vectors $\mathbf{v}$, $\mathbf{b}$ and matrix $\mathbf{A}$ are those defined in Section II. As each updating of the v_{ij} will always decrease the value of $\mathcal{E}$, the ordering and timing of the updating process will not affect the convergence. That is, each v_{ij} can be updated asynchronously. Thus, this computation structure is inherently parallel. This asynchronous property allows the computation to be implemented in analog circuit [19] for real-time surface interpolation. It can be found that the derived formula is similar to that of Gauss-Seidel matrix iterative method. However, based on this derivation, it is obvious to see that the ordering of variables and synchronization of related variables will not affect the convergence of the iteration.

B. Preconditioning by Basis Transfer

To see the effect of the basis transfer on the convergence condition of the equation system, a theoretical measure is need to examine the change of the characteristics of the system matrix. As indicated in [40], the iterative process for solving

TABLE I
CONVERGENCE RATE $-\log S(G)$ AS A FUNCTION OF RESOLUTION LEVEL J AND SURFACE SIZE

Surface Size	$J=0$	$J=1$	$J=2$	$J=3$	$J=4$
8×8	1.5491014e-03	1.4652747e-02	—	—	—
16×16	5.6147491e-04	5.6642040e-03	1.2355225e-02	—	—
32×32	3.0307722e-05	3.1554337e-04	1.8347929e-03	2.0822792e-02	—
64×64	2.3471197e-06	1.3265477e-05	4.7623176e-04	5.6534231e-03	1.0245076e-02

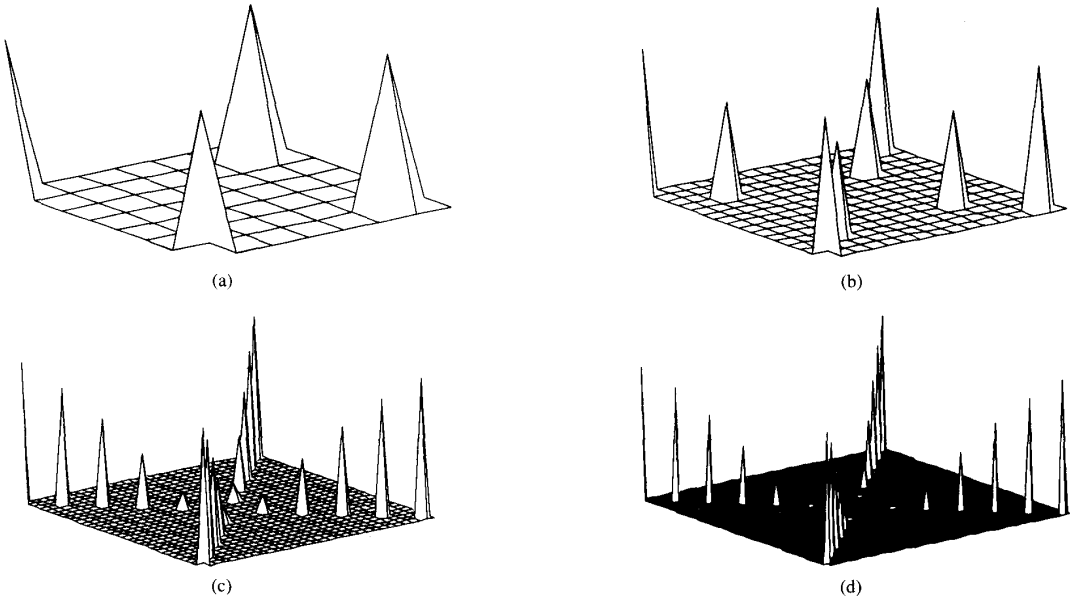

Fig. 7. The examples for testing the convergence rate. (a) 8 × 8. (b) 16 × 16. (c) 32 × 32. (d) 64 × 64.

a linear equation system $\mathbf{Av} - \mathbf{b} = 0$ can be expressed in the form as

$$\mathbf{v}^{n+1} = \mathbf{G}\mathbf{v}^n + \mathbf{k} \tag{33}$$

For the case of the above mentioned iterative computation method, the matrix $\mathbf{G}$ and the vector $\mathbf{k}$ are defined as

$$\mathbf{G} = (\mathbf{I} - \mathbf{B}_L)^{-1}\mathbf{B}_U, \quad \mathbf{k} = (\mathbf{I} - \mathbf{B}_L)^{-1}\mathbf{b}. \tag{34}$$

where $\mathbf{I}$ denotes the identity matrix, and $\mathbf{B}_L$ and $\mathbf{B}_U$ denote the strictly upper and strictly lower triangular matrices of matrix $\mathbf{B}$. The matrix $\mathbf{B}$ is defined as $\mathbf{B} = \mathbf{I} - (\mathrm{Diag}(\mathbf{A}))^{-1}\mathbf{A}$. The matrix $\mathbf{G}$ is called the iteration matrix which determines the $n+1$th solution $\mathbf{v}^{n+1}$ from the n-th solution $\mathbf{v}^n$. Denote the optimal solution of $\mathbf{v}$ as $\mathbf{v}^*$, the number of iterations required to reduce the solution error by a factor ϵ is bounded by a function of the spectral radius of matrix $\mathbf{G}$. This measure of convergence can be expressed as

$$\text{IF} \quad \|\mathbf{v}^n - \mathbf{v}^*\| < \epsilon\|\mathbf{v}^0 - \mathbf{v}^*\|, \quad \text{Then} \quad n \geq \frac{\log \frac{1}{\epsilon}}{-\log S(\mathbf{G})} \tag{35}$$

where

$$S(\mathbf{G}) \triangleq \max_{\lambda \in \mathrm{Eig}(\mathbf{G})} |\lambda|,$$
$$\mathrm{Eig}(\mathbf{G}) \triangleq \text{the set of all eigenvalues of } \mathbf{G}. \tag{36}$$

The quantity $-\log S(\mathbf{G})$ is referred to as the rate of convergence [40] and provides a measurement of the convergence condition of the iterative method. It can be seen that matrix $\mathbf{G}$ is entirely a function of the system matrix $\mathbf{A}$. Different system matrices will result in different convergence conditions. As described in Section III, the basis transfer scheme is used to transfer a system matrix $\mathbf{A}$ into a new one $\tilde{\mathbf{A}} = \mathbf{R}^T\mathbf{A}\mathbf{R}$. To verify that this transfer can result in a better convergence condition, some examples are tested. These examples are shown in Fig. 7, they are of size 8 × 8, 16 × 16, 32 × 32, and 64 × 64, respectively. In Table I, the convergence rate $-\log S(\mathbf{G})$ associated with these surface interpolation problems are listed. From Table I, it can be seen that the convergence rate increases as the resolution level J increases in all the four cases. This shows that the basis transfer scheme can be an effective preconditioner for the iterative method.

With this basis transfer scheme as a preconditioner to the proposed asynchronous iterative computation method, a fast interpolation algorithm can then be designed as the follows:

FAST INTERPOLATION ALGORITHM USING BASIS TRANSFER

Step 0. INITIATION:

(a) For a given constraint set $C_d = \{q_{ij}\}$, derive the corresponding system matrix $\mathbf{A}$ and vector $\mathbf{b}$.

(b) Chose an initial estimation vector $\mathbf{v}^0$ of the nodal variables v_{ij}'s.
(c) Chose the resolution level J and decide the matrix operators $\mathbf{D}$ and $\mathbf{R}$.

Step 1. BASIS TRANSFER:
(a) Derive the new system matrix $\tilde{\mathbf{A}} = \mathbf{R}^T\mathbf{A}\mathbf{R}$.
(b) Derive the new vector $\tilde{\mathbf{b}} = \mathbf{R}^T\mathbf{b}$.
(c) Transfer $\mathbf{v}^0$ into $\tilde{\mathbf{v}}^0 = \mathbf{D}\mathbf{v}^0$.

Step 2. ITERATIVE COMPUTATION:
(a) Set maximum iteration number MAXI and stop criterion STC. Set count = 0.
(b) For $k = 0 \sim N^2 - 1$, calculate

$$\tilde{\mathbf{v}}_{(k)}^{\text{count}+1} = \frac{-1}{\tilde{\mathbf{A}}_{(k,k)}}\left[\sum_{l=0,l\neq k}^{N^2-1}\tilde{\mathbf{A}}_{(k,l)}\tilde{\mathbf{v}}_{(l)}^{\text{count}} - \mathbf{b}_{(k)}\right]$$

(c) count = count + 1.
(d) If count > MAXI or $\mathcal{E} \leq$ STC, go to Step 3.
(e) Go to (2b).

Step 3. INVERSE TRANSFER:
(a) Transfer $\tilde{\mathbf{v}}$ back to $\mathbf{v}$ by $\mathbf{v} = \mathbf{R}\tilde{\mathbf{v}}$.
(b) Stop.

In this algorithm, the basis transfer is only applied before and after the asynchronous iterative computation method. The iterative method used in Step 2 is independent upon the algorithm. Other iterative methods can also be used. The advantage of using the chosen asynchronous iterative formula is its easy implementation. Also the asynchronous computation structure can be implemented in both serial machine and parallel analog computation network.

Compared with the direct iterative solving methods, the extra computation within this algorithm are the basis transfer in Step 1 and the inverse transfer in Step 3. Since the QMF filters are designed with the finitely supported wavelet functions, the matrix operators $\mathbf{D}$ and $\mathbf{R}$ are quite sparse. The number of the nonzero elements in each column or row of these matrices will be less than L^2, where L is the length of the QMF filter. In the case of tent function as the scaling function, the value of L^2 is less than 25. Hence, the basis transfer operations do not require much computation cost. The derivation of matrix $\tilde{\mathbf{A}}$ in (1a) is about $O(n^2)$ operations (multiplications and additions). The derivations in (1b), (1c), and (3a) are about $O(n)$ operations, respectively, where n is the number of the nodal variables v_{ij}'s. So, the extra computation for basis transfer is mainly the operation in (1a). Roughly, the computation cost required for the basis transfer is about the amount of computation needed for L^2 iterations (the amount of computation for one iteration in Step 2 is about $O(n^2)$ operations). Hence, when the size of the interpolated surface is large, this portion of computation is negligible.

V. Experiments and Analysis

A. Experimental Results

Some experiments are shown in the following to demonstrate the performance of the proposed method. In these experiments, the value of β is set to 10 such that the resulted surfaces will fit the given constraints closely. The initial estimation of the interpolated surface is derived by a simple zero estimation method. It sets all the variables to zero initially except those constrained variables which are set to the known depth values of the constraint data. In each of the convergence curves, logarithm of the objective function is used to denote the convergence status of the computation.

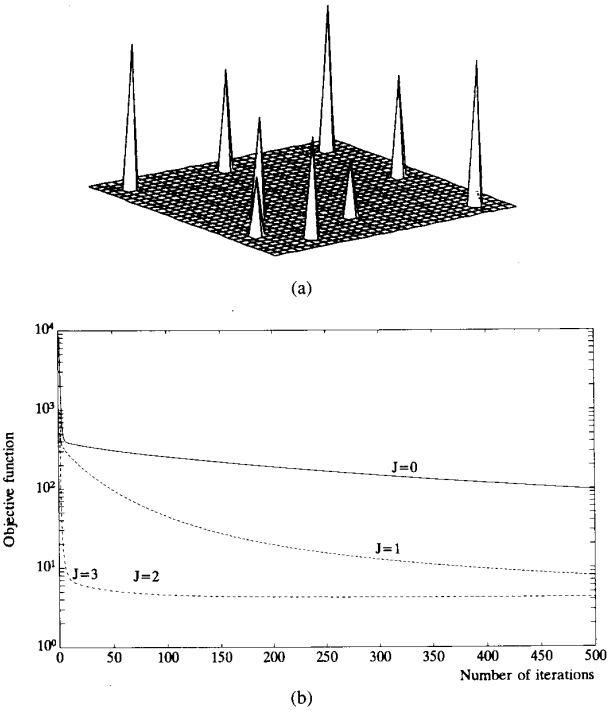

Fig. 8. The first experiment of the fast surfaceinterpolation algorithm. (a) The initial surface. (b) The convergence curves.

In the first example, the constraints density is only 0.89% (i.e., there are 9 constrained variables among 1024 unknown variables). The initial surface using zero estimation method is shown in Fig. 8(a). The convergence of the objective energy function with the proposed method using different resolution levels (J) is plotted in Fig. 8(b). The corresponding interpolated surfaces with different resolution levels after 500 iterations are shown in Fig. 9. The topmost curve ($J = 0$) in Fig. 8(b) denotes the convergence status using direct iterative computation without preconditioning. It can be found that the convergence rate is significantly improved when the basis transfer scheme is applied ($J = 1, 2, 3$). In the second example, a saddle surface is interpolated. The initial surface is shown in Fig. 10(a). In this example, the constraint density is 18.3%. The convergence of the objective energy function using different resolution levels (J) are shown in Fig. 10(b). Similar to the first example, the proposed algorithm can improve the convergence rate significantly. Fig. 11 shows the surfaces interpolated with the proposed method using different resolution levels after 100 iterations.

To compare with other acceleration schemes, both the the multi-grid method [35], [37] and the hierarchical basis method

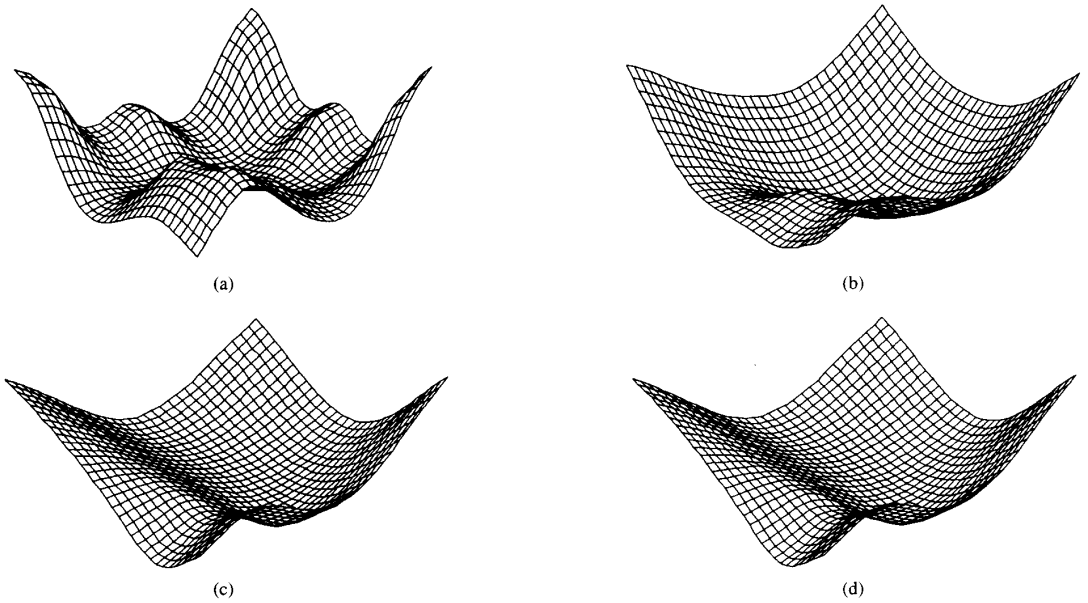

Fig. 9. The results of the firstexperiment after 500 iterations. (a) $J = 0$. (b) $J = 1$. (c) $J = 2$. (d) $J = 3$. (J: the resolution level).

[39] are tested. For the problem with given constraints described in Fig. 12(a), the convergence of the objective energy function by the multigrid method and the proposed basis transfer method are plotted in Fig. 12(b). The results of the two methods after 300 iterations are shown in Fig. 13. In this example, only two resolution layers are used in the multigrid method since the implementation of the multigrid method is quite complicated. In Fig. 12(b), the convergence curve by using the multigrid method is oscillatory. The oscillation is due to the inconsistency of the energy function between the coarse and fine levels. As shown in Fig. 12(b), with the same two levels of decomposition ($J = 1$), the proposed basis transfer method seems to perform better than the multigrid method. As for the complexity in the implementation of both algorithms, the basis transfer method is comparatively simpler.

In the last example with given constraints described in Fig. 14(a), the convergence performances by both the hierarchical basis method and the proposed basis transfer method are shown in Fig. 14(b). The curves marked as $L = 1 \sim 6$ are the results obtained by applying the hierarchical basis scheme [39] as the preconditioner. The value of L stands for the number of the smoothing levels. When $L = 1$, no preconditioning is applied. This is equivalent to the case of $J = 0$ in the basis transfer method. As shown in Fig. 14(b), when preconditioning is applied ($J = 1 \sim 3$ and $L = 2 \sim 6$), both methods can significantly improve the convergence rate. However, the basis transfer method is more efficient, the amount of improvement from one level to its next level is larger. Comparing the best cases of the two methods, the result of the basis transfer method with $J = 3$ is better than the result of the hierarchical basis method with $L = 4$.

The hierarchical basis method has been applied by Szeliski [34] in surface interpolation. In Szeliski's approach, the conjugate gradient search was used in the iterative computation.

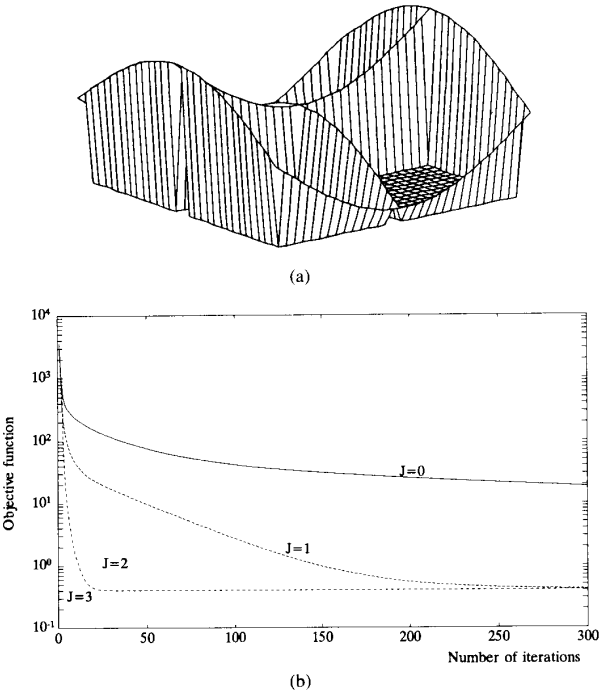

Fig. 10. The second experiment of the fast surface interpolation algorithm. (a) The initial surface. (b) The convergence curves.

In Fig. 14(c), the curves marked as $S = 1 \sim 6$ are the results obtained with the hierarchical basis scheme as the preconditioner and the conjugate gradient as the iterative computation method. The value of S stands for the number of the smoothing levels. When $S = 1$, no preconditioning is applied. The difference between the S curves in Fig. 14(c) and the L curves

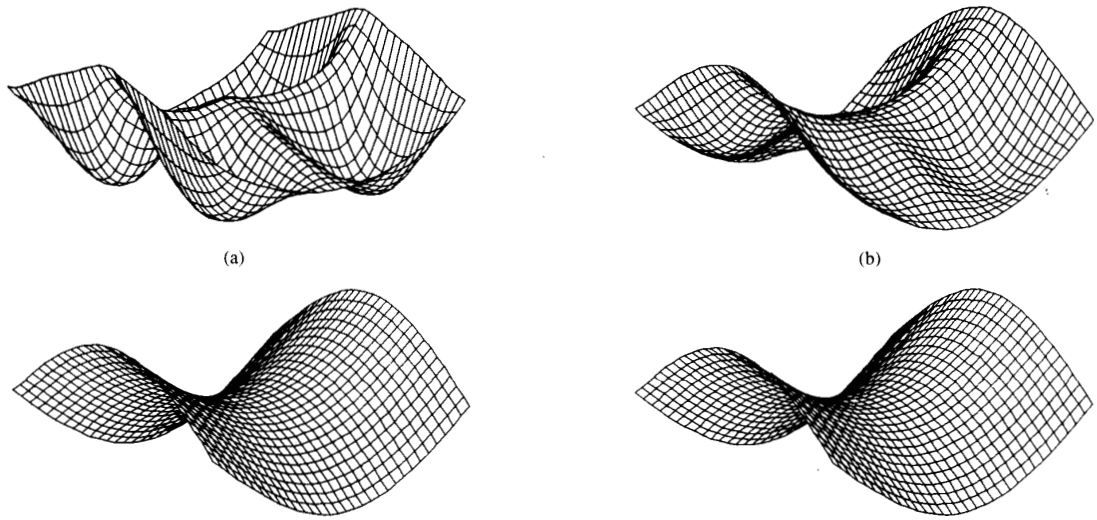

Fig. 11. The results of the second experiment after 100iterations. (a) $J = 0$. (b) $J = 1$. (c) $J = 2$. (d) $J = 3$. (J: theresolution level).

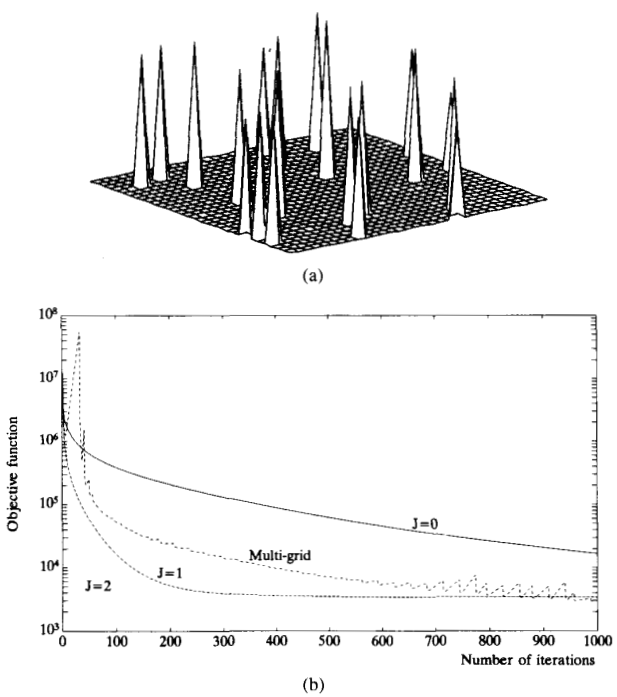

Fig. 12. The third experiment forcomparing with the multigrid method. (a) The initial surface. (b) The convergence curves of the basis transfer method and themulti-grid method.

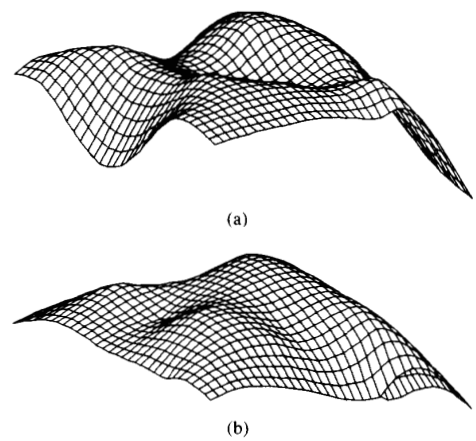

Fig. 13. The results of the thirdexperiment after 300 iterations. (a) Multigrid method. (b) Basis transfer method ($J = 1$).

in Fig. 14(b) are due to the different numerical computation methods. It is well known that the conjugate gradient method is inherently faster than the general iterative methods. However, when preconditioning is applied ($S = 2 \sim 6$ and $L = 2 \sim 6$), the improvement in convergence is more significant with the asynchronous computation method. This example indicates the fact that the simple iterative method such as Gauss–Seidel can be made to work better than the complex conjugate gradient method when proper multiresolution preconditioning is applied. The results by the basis transfer method ($J = 3$) and the hierarchical basis method ($L = 6$ and $S = 6$) after 30 iterations are shown in Fig. 15. From the convergence curves in Fig. 14(b)–(c), it can been found that the performance of the interpolation can be more affected by the preconditioner than the subsequent iterative computation methods.

B. Analysis

The above examples indicate that the convergence rate of surface interpolation can be significantly improved by the proposed basis transfer algorithm. This improvement of convergence is due to the use of bases at different resolution levels. Through the basis transfer, the original nodal variables $\mathbf{v}$ are converted to the combination of its low-frequency component $\mathbf{v}_J$ and its high-frequency components

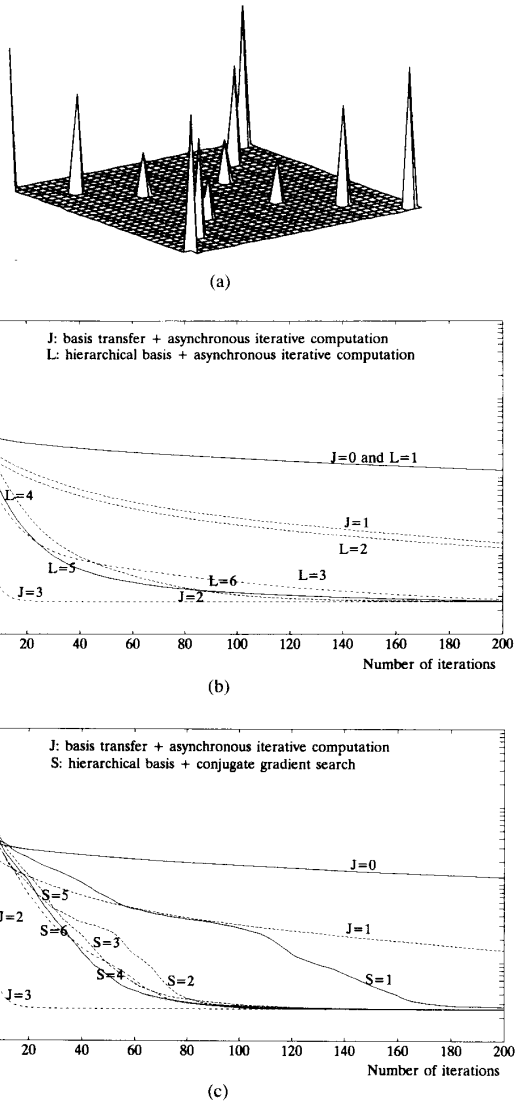

Fig. 14. The fourth experiment for comparing with the hierarchical basismethod. (a) The initial surface. (b) The convergence curves ofthe basis transfer method and the hierarchical basis method(using asynchronous iterative computation). (c) The convergence curves of the basis transfer method and the hierarchical basismethod (using conjugate gradient search computation).

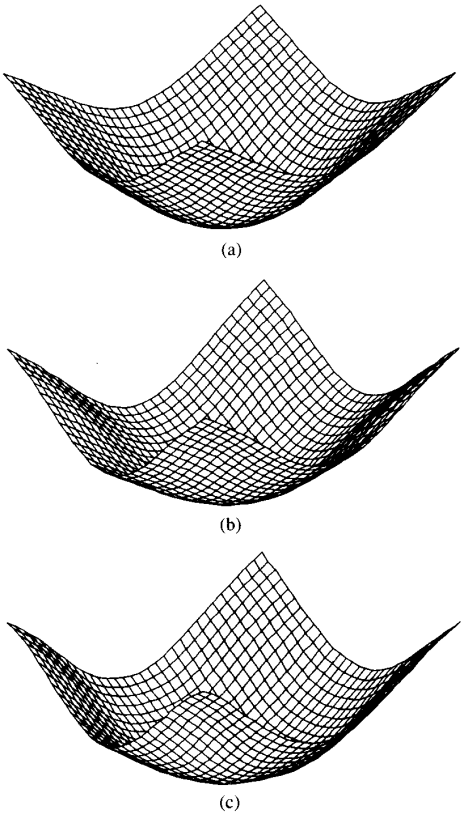

Fig. 15. The results of the fourth experiment after 30 iterations. (a) Basis transfer method ($J = 3$). (b) Hierarchical basis method $L = 6$ (asynchronous iterative computation). (c) Hierarchical basis method $S = 6$ (conjugate gradient search computation).

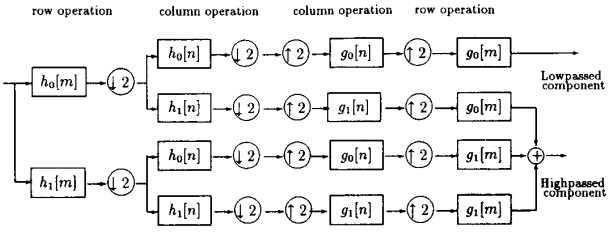

Fig. 16. The 2-D filter banks for error analysis.

$\mathbf{w}_j^i$,$(j=1\sim J, i=1,2,3)$. The use of basis transfer has greater effect on the low-frequency component, thus the low-frequency error in the iteration can then be effectively reduced. To verify this inference, the error in the computation of the second example (Fig. 10) is analyzed.

For this, the result obtained by using the proposed algorithm after 1000 iterations (with $J = 3$) is set as the reference solution $\mathbf{v}^*$. In each iteration, the result $\tilde{\mathbf{v}}$ is transferred back to $\mathbf{v}$ to compare with the reference surface $\mathbf{v}^*$. To extract the low-frequency component and the high-frequency component of a surface, a 2-D filter banks described in Fig. 16 is used. The filters in this filter banks are those listed in Fig. 5. With this filter banks, the reference surface $\mathbf{v}^*$ and the surface $\mathbf{v}$ obtained in each iteration can be decomposed into their low-frequency and high-frequency components, respectively (Fig. 17). The low-frequency and high-frequency components of the reference surface $\mathbf{v}^*$ are shown in Fig. 18. In each iteration, the difference between the solution $\mathbf{v}$ and reference surface $\mathbf{v}^*$ is evaluated as the error. The low-frequency and high-frequency components of the error can then be obtained by passing the error through the 2-D filter banks.

In Fig. 19, the energy (i.e., the vector norm) of the two error components for the first 500 iterations are shown. It can be found that the high-frequency error is relatively small and attenuate very fast whether the basis transfer scheme is applied or not. However, the attenuation speed of the low-frequency

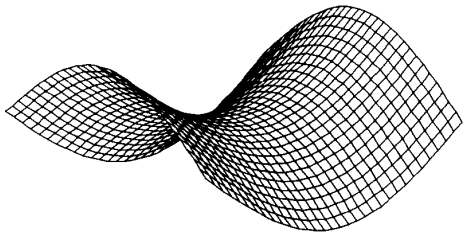

Fig. 17. The reference surface for error analysis.

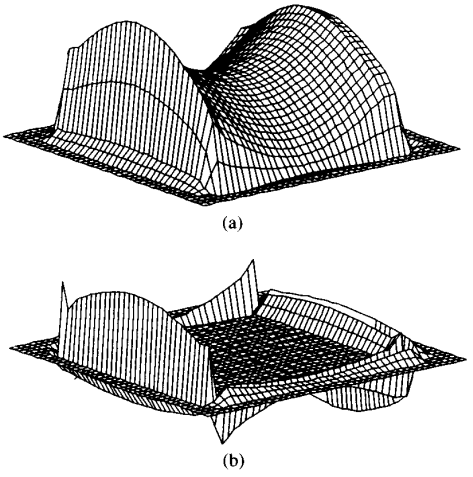

Fig. 18. The low-frequency component and the high-frequency component of the reference surface. (a) Low-frequency component. (b) High-frequency component.

error is obviously increased when the basis transfer scheme is used. This indicates that the convergence rate is dominated by the low-frequency portion of the surface and can be effectively improved by using basis of larger support. By emphasizing the low-frequency component of the nodal variables (extracting the low-frequency component $\mathbf{v}_J$ from $\mathbf{v}$), the convergence can then be accelerated. That is, if the low-frequency portion converge faster, the entirely surface will converge faster.

The effect of the basis transfer can also be observed from the convergence of the converted nodal variables $\{\mathbf{v}_J, \mathbf{w}_j^i\}$. To examine the convergence condition of these variables, we partition these variables into two groups $VJ \triangleq \{\mathbf{v}_J\}$ and $WJ \triangleq \{\mathbf{w}_j^i{}_{,(j=1\sim J, i=1,2,3)}\}$. In each iteration, the variation of these two groups of variables are evaluated. The energy (vector norm) of the variation of these two groups of variables for the first 500 iterations are plotted in Fig. 20. Fig. 20(a) shows the variation of the original nodal variables. Since no conversion of nodal variables is used, only one group of variables is analyzed. Fig. 20($b \sim d$) show the variations of the two groups of variables at resolution level $J = 1, 2, 3$, respectively. From Fig. 20, it can be found that the variations of the group WJ at resolution level $J = 1, 2, 3$ are very similar. This indicates that the high-frequency portion of the interpolation problem converges quite quickly and is not much affected by the basis transfer scheme. In the other hand, the variation of the group VJ is decreased faster in the iteration when the value of J is increased. This indicates that the low the convergence is

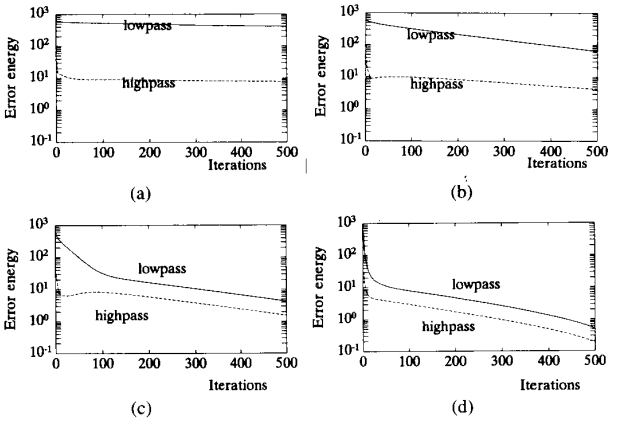

Fig. 19. The energy of the low-frequency error and the high-frequency errorcomponent. (a) $J = 0$. (b) $J = 1$. (c) $J = 2$. (d) $J = 3$.

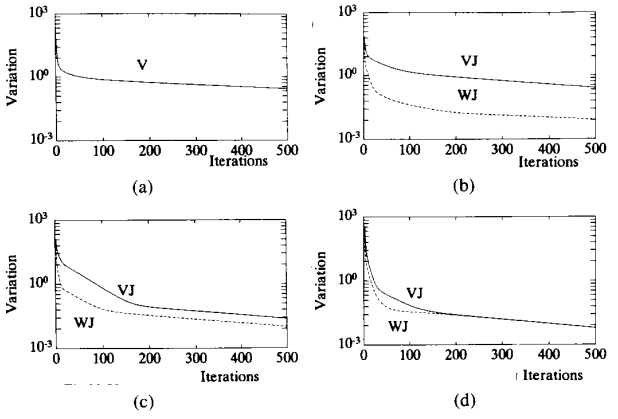

Fig. 20. The variation of the variable groups VJ and WJ. (a) $J = 0$. (b) $J = 1$. (c) $J = 2$. (d) $J = 3$.

dominated by the low-frequency portion of the interpolation problem can be effectively improved with multiresolution preconditioning. When more resolution levels (larger J) are used, the number of variables in group VJ will also decrease. This will also influence the status of convergence in addition to the use of larger supported basis.

In the above experiments, the weighting factor β is set at 10. The results indicate that the convergence rate is increased when the number of resolution levels J is increased. But, when the weighting factor β is set at a large value, this trend is no longer true. This fact was also pointed out by Szeliski [34] in his implementation of the hierarchical basis method. This is to say that, when the cost functional is emphasized, the optimal value of J for fastest convergence does not correspond to the largest resolution layers. This is a problem deserving further research. However, based on our experience, unless the value of β is greater than 50, the above mentioned problem will not exist. Hence, if the weighting of the cost functional is less than 50, one can always use the largest J as the optimal choice.

In applying the multiresolution wavelet transform, the treatment of the boundary condition needs special attention. In order for the interpolated surface stable in the boundary, extra nodes outside the domain of interest are added. The values of

these extra nodes are constrained by certain measure such as smoothness, symmetry etc. For this, additional equations are used to establish the relationship among the extra nodes and the nodes inside the domain of interest. The number of extra nodes that are to be inserted depends on the order of the basis function. A detailed discussion of this issue can be found in [18]. Due to the cardinal property, the boundary condition for the tent functionin is simple. In the case of tent function for surface interpolation, the treatment of the boundary condition can be found in [19], [20]. In summary, the treatment of boundary condition depends on the order of the basis function and the functional form of the regularization. Care is needed to take into account the overlapping condition of the basis functions and their derivatives. The overall effect is reflected in the relation coefficients t_{ijmn}'s.

The tent basis used in our experiments is the first order B-spline function. The cardinal property of the triangular function can simplify the manipulation in the discretization of the interpolation problem. Beside the triangular function, various interpolation basis functions can also be applied. Interpolation using spline functions of different orders has been studied in [18]. In wavelet transform, use of spline function as the scaling function has been well developed in the study of biorthogonal wavelet transform [7]. This is a generalization of the conventional orthogonal wavelet transform. By relaxing the constraint on orthogonality, biorthogonal wavelet transform has more freedom in the design of wavelets with good spatial-spectral localization. Also, it is possible to design symmetric scaling function and wavelet under the perfect decomposition/reconstruction requirement. This is not possible for the orthogonal wavelet transform except in the trivial Harr space case. These characteristics of the biorthogonal wavelet transform make it a powerful tool in dealing with the interpolation problem.

Use of wavelet transform to precondition the surface interpolation problem can also be found in [29], [30]. In Pentland's approach, discrete wavelet transform is directly applied to diagonalize the linear equation system of the discretized interpolation problem. With this diagonal preconditioning, he has shown a way to obtain fast solution with fewer iterations by approximating the off-diagonal terms of the preconditioned equation system with zero. This approach can be treated as a pure algebraic operation to rotate the coordinate system. This is different from the scheme of multiresolution wavelet signal representation proposed in this paper. A more detailed treatment of the mathematical theory behind the diagonal preconditioning by wavelet transform can be found in [21]. This diagonalization property has been considered as an important characteristic of the wavelet preconditioning scheme. However, to directly diagonalize the equation system, the filter bank associated with the discrete wavelet transform has to be carefully designed. Also, the structure of the system matrix needs be considered. For the surface interpolation problem, the effect of diagonalization will also depends on the weighting of the cost functional. Since, when the weighting is large, the effect of the diagonalization is not obvious and significant errors will be introduced [30]. This remains an interesting issue deserves further attention.

VI. Conclusion

In this paper, a fast surface interpolation algorithm using basis transfer scheme has been proposed. The basis transfer scheme is developed from the multiresolution signal representation technique in the wavelet transform. Applying the basis transfer scheme as a preconditioner, significant improvement in the convergence rate of the proposed asynchronous iterative solving method for the surface interpolation is obtained. The inherent parallel computation structure of the asynchronous iterative solving method can also be implemented with the analog circuit for fast computation. Comparison of the proposed algorithm with the multi-grid method and the hierarchical basis method has also been presented. From the experiment results, the performance of the proposed algorithm has been shown to be better in the surface interpolation problem.

Since, the basis operation of the proposed algorithm is simple, multiresolution basis can be more systematically generated. The basis transfer scheme is only required before and after any iterative solving method. Computation can be carried out at proper connection level such that highest computation speed can be obtained. Application of this proposed method to different problems are being considered. Also, detailed analysis of the relationship between the issues of signal representation in different resolution by different wavelet bases and the computation with different nodal connection are being studied.

Acknowledgment

The authors would like to express their gratitudes to the reviewers for their most helpful comments on this paper.

References

[1] A. Aldroubi, M. Unser, and M. Eden, "Discrete spline filters for multiresolutions and wavelet of l_2," BEIP/National Center for Res. Resources, Rep. No. 21/91, 1991.

[2] O. Axelsson and V. A. Barker, *Finite Element Solution of Boundary Value Problems: Theory and Computation*. Orlando, FL: Academic, 1984.

[3] A. Brandt, "Multi-level adaptive solutions to boundary-value problems," *Math. Computat.*, vol. 31, pp. 333–390, 1977.

[4] M. T. Chiaradia, A. Distante, and E. Stella, "Three-dimensional surface reconstruction integrating shading and sparse stereo data," *Optic Eng.*, vol. 28, no. 9, pp. 935–942, 1989.

[5] C. K. Chui, *An Introduction to Wavelets*. Boston, MA: Academic Press, Boston, 1992.

[6] ——, "On compactly supported spline wavelets and a duality principle," *Trans. Amer. Math. Soc.*, vol. 330, no. 2, pp. 903–915, 1992.

[7] A. Cohen, I. Daubechies, and J.-C. Feauveau, "Biorthogonal bases of compactly supported wavelets," *Commun. Pure Appl. Math.*, to appear.

[8] I. Daubechies, "Orthonormal bases of compactly supported wavelets," *Commun. Pure Appl. Math.*, vol. XLI, pp. 909–996, 1988.

[9] R. D. Eastman and A. M. Waxman, "Using disparity functionals for stereo correspondence and surface reconstruction," *Comput. Vision Graphics Image Processing*, vol. 39, pp. 73–101, 1987.

[10] W. E. L. Grimson, "An implementation of a computational theory of visual surface interpolation," *Comput. Vision Graphics Image Processing*, vol. 22, pp. 39–69, 1983.

[11] ——, "Computational experiment with a feature based stereo algorithm," *IEEE Trans. Pattern Anal. Machine Intell.*, vol. PAMI-7, no. 1, pp. 17–34, 1985.

[12] C. W. Groetsch, *The Theory of Tikhonov Regularization for Fredholm Equations of the First Kind*. Boston, MA: Pitman, 1984.

[13] W. Hackbusch, *Multi-Grid Methods and Applications*. New York: Springer-Verlag, 1985.

[14] W. Hackbusch and U. Trottenberg, Eds., *Multigrid Methods*. New York: Springer-Verlag, 1982.

[15] L. A. Hageman and D. M. Young, *Applied Iterative Methods*. New York: Academic Press, 1981.
[16] W. Hoff and N. Ahuja, "Surfaces from stereo: Integrating feature matching, disparity estimation, and contour detection," *IEEE Trans. Pattern Anal. Machine Intell.*, vol. PAMI-11, no. 2, pp. 121–136, 1989.
[17] H. C. Hsieh and W. T. Chang, "Computation network for visible surface reconstruction," in *Proc. SPIE Conf. Visual Commun. Image Processing*, Lausanne, Switzerland, 1990, pp. 1504–1515.
[18] W. T. Chang, H. C. Hsieh, and W.-Hsing Lai, "Second order smoothness measure in curve fitting," in *Proc. Telecommun. Symp.*, Hsinchu, ROC, 1990, pp. 550–555.
[19] H. C. Hsieh and W. T. Chang, "Analog computation structure for surface reconstruction," *J. Visual Commun. Image Represent.*, vol. 2, no. 4, pp. 381–394, 1991.
[20] ——, "Multi-layer computation structure for surface reconstruction," *IEEE Trans. Image Processing*, submitted.
[21] S. Jaffard, "Wavelet methods for fast resolution of elliptic problems," *SIAM J. Numerical Anal.*, vol. 29, no. 4, pp. 965–986, 1992.
[22] D. R. Kincaid and L. J. Hayes, *Iterative Methods for Large Linear Systems*. New York: Academic Press, 1990.
[23] P. Lancaster and K. Salkauskas, *Curve and Surface Fitting*. New York: Academic Press, 1986.
[24] M. M. Lavrentev, V. G. Romanov, and S. P. Shishatskii, "Ill-posed problems of mathematical physics and analysis," *Amer. Math.*, Providence, RI, 1986.
[25] G. G. Lorentz, C. K. Chui, and L. L. Schumaker, Eds., *Approximation Theory*. New York: Academic Press, 1976.
[26] S. G. Mallat, "A theory for multiresolution signal decomposition: The wavelet representation," *IEEE Trans. Pattern Anal. Machine Intell.*, vol. PAMI-11, no. 7, pp. 647–693, 1989.
[27] ——, "Multifrequency channel decompositions of images and wavelet models," *IEEE Trans. Signal Processing*, vol. 37, no. 12, pp. 2091–2110, 1989.
[28] D. Marr, *Vision: A Computational Investigation into the Human Representation and Processing of Visual Information*. San Francisco, CA: Freeman, 1982.
[29] A. P. Pentland, "Surface interpolation networks," *Neural Computat.*, vol. 5, no. 3, pp. 430–442, 1993.
[30] ——, "Interpolation using wavelet bases," *IEEE Trans. Pattern Anal. Machine Intell.*, vol. 16, no. 4, pp. 410–414, Apr. 1994.
[31] P. R. Prenter, *Spline and Variational Methods*. New York: John Wiley, 1975.
[32] K. Rektorys, *Variational Methods in Mathematics, Science, and Engineering*, second ed. Dordrecht, The Netherlands: Reidel, 1980.
[33] M. B. Ruskai, R. Coifman, Y. Meyer, *et al.*, *Wavelets and Their Applications*. Boston, MA: John and Bartlett, 1992.
[34] R. Szeliski, "Fast surface interpolation using hierarchical basis functions," *IEEE Trans. Pattern Anal. Machine Intell.*, vol. PAMI-12, no. 6, pp. 513–528, 1990.
[35] D. Terzopoulos, "Multi-level computational processes for visual surface reconstruction," *Comput. Vision Graphics Image Processing*, vol. 24, pp. 52–96, 1983.
[36] ——, "Regularization of inverse visual problems involving discontinuities," *IEEE Trans. Pattern Anal. Machine Intell.*, vol. PAMI-8, no. 4, pp. 413–424, 1986.
[37] ——, "Image analysis using multigrid relaxation methods," *IEEE Trans. Pattern Anal. Machine Intell.*, vol. PAMI-8, no. 2, pp. 129–139, 1986.
[38] ——, "The computation of visible-surface representations," *IEEE Trans. Pattern Anal. Machine Intell.*, vol. PAMI-10, no. 4, pp. 417–438, 1988.
[39] H. Yserentant, "On the multi-level splitting of finite element space," *Numerische Mathimatik*, vol. 49, pp. 379–412, 1986.
[40] D. M. Young, *Iterative Solution of Large Linear Systems*. New York: Academic Press, 1971.

Ming-Haw Yaou was born in Taiwan on January 5, 1965. He received the B.S. degree in 1987 and the M.S. degree in 1989 both from the Department of Communication Engineering, National Chiao-Tung University, Hsinchu, Taiwan. Currrently, he is working toward the Ph.D. degree in the Department of Electronics Engineering, National Chiao-Tung University.

His research interests include digital communications, computer vision, and digital signal processing.

Wen-Thong Chang was born in Taiwan on November 15, 1956. He received the B.S. degree from the Department of Communication Engineering, National Chiao-Tung University, Hsinchu, Taiwan in 1979, and the Ph.D. degree from the Department of Electrical Engineering, Carnegie-Mellon University, Pittsburgh, PA in 1985.

Currently, he is an Associate Professor in the Department of Communication Engineering, National Chiao-Tung University, Hsinchu, Taiwan. His research interests include digital signal processing, digital image processing, computer vision, and video compression.